COMSOL
CONFERENCE
2024 BOSTON

A Digital Twin Approach for Electric Vehicle Battery Management Systems

Roger Painter [1,*], Ranganathan Parthasarathy [1], Lin Li [1], Irucka Embry [2], Lonnie Sharpe [3] and S. Keith Hargrove [4]

1 Department of Civil Engineering, Tennessee State University, Nashville, TN 37209, USA; rpainter@tnstate.edu;
2 Department of Civil Engineering, Tennessee State University, Nashville, TN 37209, USA; rparthas@tnstate.edu ;
3 Department of Civil Engineering, Tennessee State University, Nashville, TN 37209, USA; lli1@tnstate.edu
4 EcoC²S, Nashville, TN 37206, USA; iembry@my.tnstate.edu
5 Department of Mechanical Engineering, Tennessee State University, Nashville, TN 37209, USA; sharpe@coe.tsuniv.edu
6 Tuskegee University, Tuskegee, AL 36088, USA; skhargrove@gmail.com
* Correspondence: rpainter@tnstate.edu

Abstract

The emerging digital twin vision for computer simulation encompasses the entire lifecycle of real-world applications and products. The digital twin concept enables the integration of complex multiphysics and multiscale models and simpler reduced order models (ROM). The multiphysics models store current expert engineering knowledge that is accessible and reusable by non-experts at all stages of the products lifecycle via locally implemented or on-board ROM. Furthermore, the ROM can provide real time operational and control capabilities that are subject to verification and updating by the off-board multiphysics model. Our approach to developing a digital twin simulation of lithium-ion batteries for electric vehicles utilized a dataset generated from the COMSOL® Multiphysics simulation of the Cahn-Hilliard equation for a single particle model (SPM) of a lithium iron phosphate (LiFePO4) cathode. The SPM cannot simply be scaled up to bulk scale processes, so we took a machine learning (ML) approach to derive latent variables from the data. We relate the SPM simulation statistically to the battery cell voltage and temperature responses. Specifically, the plateauing effect of the battery's voltage response at higher ambient temperatures and the apparent diffusion-controlled behavior at lower temperatures are related by statistical inference to the SPM. The simulation dataset was first subjected to singular value decomposition (SVD) and principal component analysis (PCA) to identify latent variables and for model order reduction. The ROM was then developed by utilizing the reduced order simulation dataset and experimental data for an A123 Systems 26650 2.3 Ah cylindrical battery to train a self-normalizing neural network (SNN). Finally, the ROM was verified as an on-board battery management system (BMS) for ambient temperatures ranging from 253 to 298 K and discharge rates ranging from 1 C to 20.5 C.

Keywords: lithium-ion batteries; LIB; $LiFePO_4$; electric vehicles; Cahn–Hilliard; principal component analysis, neural networks

1. Introduction

There is an ongoing global trend of electrifying transportation, and as a result, intensive research is underway into electric and hybrid electric vehicles (EVs and HEVs) [1,2]. Lithium-ion batteries have become the most promising choice for EVs due to their high energy density and long cycle life [3,4]. Battery management systems (BMSs) are necessary for EV applications to prevent Li-ion batteries from overheating and overcharging and to avoid potential thermal runaway. Currently, BMS cannot store and process large amounts of data while managing the battery's state of charge (SOC), voltage, and temperature in real-time [5-7]. To address this shortcoming, additional research is needed to develop reduced-order models (ROM) that can both model complex battery mechanisms and provide real-time management data. Applications of machine learning (ML) and artificial intelligence (AI) are fertile areas for eventual solutions to this problem.

Models that describe battery dynamic processes at all levels are not feasible. Therefore, mechanistic battery models, referred to as full-order models (FOM), need to be tailored to specific purposes that require a deep understanding of a particular aspect of the battery's operation and performance. Many mechanistic models have been developed specifically to describe battery thermal behavior [8–11]. In general, models for analysis and diagnosis purposes employ detailed simulations of the battery's physics and, thus, are often multidimensional, multiphysics models and are computationally slow. Models for control and optimization applications are usually computationally fast but provide a limited

description of the underlying physics. Decades of research have been conducted to develop reduced-order models (ROMs) that adequately retain robustness without excessive computational complexity. The state of the art for the various methods of achieving Li-ion battery ROM has recently been reviewed in the literature [12]. We limit our following discussion of such methods to equivalent circuit models (ECMs), their model-based extensions, and the single-particle model approximation. These methods are most pertinent since our ROM, developed in the following sections, is a single-particle application and is most likely to be used instead of or alongside an ECM.

ECMs that do not consider fundamental physics have been extensively used to imitate the relationships between battery input and output systems while offering real-time computation. ECM use electrical circuits to simulate lithium-ion cells utilizing capacitors to shape the battery capacity, while variable resistors and controlled-voltage sources shape the temperature effect or SOC variations.

Lithium iron phosphate ($LiFePO_4$) is the most frequently used phosphate-based cathode material in Li-ion batteries. $LiFePO_4$ has a strong tendency to separate into solid high-Li+-concentration and low-Li+-concentration phases, leading to the battery's characteristic broad voltage plateau at room temperature. See Figure 1.

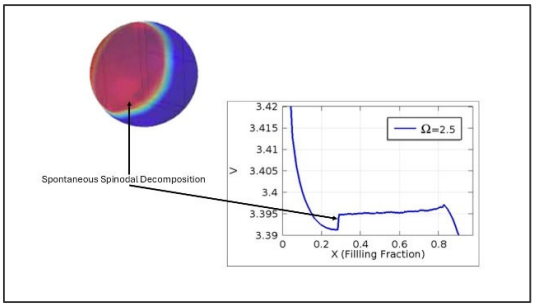

Figure 1. Depiction of separation into high Li^+ concentration phase and low Li^+ concentration phase.

Traditionally, mathematical models of intercalation dynamics in $LiFePO_4$ cathodes were based on spherical diffusion or the shrinking core concept However, recent experimental and theoretical progress suggests that a more realistic SPM should encompass a phase field model for equilibrium and nonequilibrium solid-solution transformations. Our ROM was motivated by (Zeng & Bazant, 2013), and the spatial mass transfer elements of our 3-D COMSOL® Multiphysics finite element solution are similar to their 1-D, isotropic, and isothermal solution [13-15]. The major enhancement of our single-particle model (SPM) is that it is a multiphysics thermal model that fully couples the battery cell's heat transfer model. Statistically, we relate the SPM simulation to battery cell property estimation. Specifically, the plateauing effect of the battery's voltage response at higher ambient temperatures and the apparent diffusion-controlled behavior at lower temperatures are related to the SPM by statistical inference. The ROM was realized by subjecting the raw simulation results from the COMSOL® Multiphysics simulation data to principal component analysis (PCA) to determine the lowest-order simulation dataset capable of fitting the experimental data using a self-normalizing neural network (SNN). We validated our SPM based on available experimental data for the A123 Systems 26650 2.3 Ah battery.

2. Methods and Materials

Our approach to developing a digital twin simulation of lithium-ion batteries for electric vehicles utilized a dataset generated from the COMSOL® Multiphysics simulation of the Cahn-Hilliard equation for a single particle model (SPM) of a lithium iron phosphate (LiFePO4) cathode. The SPM cannot simply be scaled up to bulk scale processes, so we took a machine learning (ML) approach to derive latent variables from the data. The simulation dataset was first subjected to singular value decomposition (SVD) and principal component analysis (PCA) to identify latent variables and for model order reduction. The ROM was then developed by utilizing the reduced order simulation dataset and experimental data for an A123 Systems 26650 2.3 Ah cylindrical battery to train a self-normalizing neural network (SNN). The value of our approach is realized in conjunction with a digital-twin (DT) configuration with an offboard COMSOL® Multiphysics SPM simulation, allowing the ROM to be periodically updated by retraining the SNN for aging batteries and actual operating conditions.

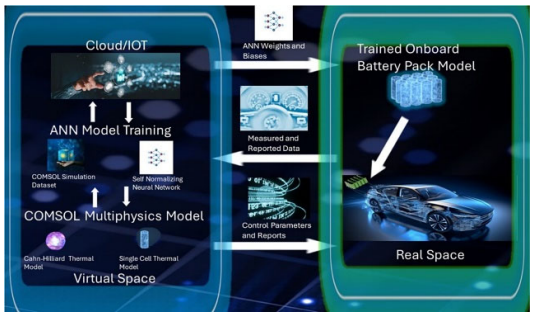

Figure 2. Visual abstract for how our BMS fits into the EV automation infrastructure.

In this configuration, only the trained SNN is onboard and in real time. Our approach to implementing a DT for lithium-ion batteries follows the process of (Singh et al. [16], 2021) See Figure 2.

2.1 Theory and Simulation

Our SPM poses the Cahn–Hilliard equation in COMSOL® Multiphysics' standard PDE format as

two coupled second-order PDE in ion concentration and chemical potential, respectively. In our SPM we assumed the particles to be spherical and isotropic. See Figure 3. The model equations are given below, where the overbar denotes dimensionless parameters and variables. We provide only the main points of the derivation of the Cahn–Hilliard equation and refer the reader to (Zeng & Bazant, 2013) for more details. The diffusional chemical potential based on the regular solution model and acquired from the Cahn–Hilliard free energy functional is

$$\bar{\mu} = -k_b T\, ln\left[\frac{\bar{c}}{1-c_m}\right] + \frac{\tilde{\Omega}(c_m-\bar{c})}{c_m} - \frac{KV_S}{c_m}\bar{\nabla}^2\bar{c} \quad (1)$$

The basic equation of evolution for mass conservation is

$$\frac{\partial \bar{c}}{\partial t} = -\bar{\nabla}\cdot\bar{q} \quad (2)$$

The ion flux is driven by the gradient of the diffusional chemical potential as

$$\bar{q} = \frac{-D_0(c_m-\bar{c})}{k_m T c_m}\bar{\nabla}\bar{\mu} \quad (3)$$

Voltage enters the Cahn–Hilliard SPM through Butler–Volmer kinetics obtained from transition state theory for concentrated solutions as

$$I = I\left[exp(-\alpha\bar{\eta})\, i - exp\big((1-\alpha)\bar{\eta}\big)\right] \quad (4)$$

Where α is the electron transfer symmetry factor, $\eta = \Delta\varphi - \Delta\varphi_{eq}$ is the surface overpotential because of the activation polarization, $\Delta\varphi$ is the local voltage drop across the interface, and $\Delta\varphi_{eq}$ is the Nernst equilibrium voltage. Transient temperature response and thermal power conservation were incorporated into the ROM by an enthalpy balance on the bulk battery. An A123 Systems 26650 2.3 Ah cylindrical battery was selected because it is extensively studied, and property data are readily available.

A cylindrical Li-ion battery is constructed by rolling a stack of cathode/separator/anode layers. The individual layered sheets are thin, and lumped parameters are used. Therefore, material properties such as thermal conductivity, density, and specific heat capacity are presumed to be constant in a homogeneous and isotropic body. In the axial direction, the thermal conductivity is one or two orders of magnitude higher than in the radial direction, leading to a uniform temperature distribution in the axial direction. Additionally, considering natural convection, the heat transfer at the surface is much smaller than the internal heat transfer by conduction, leading to negligible temperature gradients inside the battery. Based on these assumptions, the energy balance equation in the battery can be expressed by one bulk volume-averaged temperature. To estimate the thermal response of the battery, we utilized a simplified energy balance equation for the enthalpy change for electrochemical reactions. Assuming a constant system volume and pressure and neglecting heat generation because of enthalpy of mixing, the energy balance equation is

$$Mc_p\frac{\partial T}{\partial t} = I\left(V_{OC} - T\frac{\partial V_{OC}}{\partial T}\right) - IV + \dot{q}_{sur} \quad (5)$$

The term $T\frac{\partial V_{OC}}{\partial T}$ stands for reversible heat generation and can be calculated from the entropy of the reaction. In this study, this reversible heat generation was ignored for simplicity. Assuming this simplification, the OCV becomes a function of SOC only, and Equation (5) was solved exactly for the battery's temperature response for initial temperatures given by the COMSOL® parameter sweep data.

$$T(t) = T_{surr} - \frac{exp\left(-\frac{A_b h_c t}{c_p v \rho}\right)\left(-1+exp\left(\frac{A_b h_c t}{c_p v \rho}\right)\right) I_b(\bar{V}(T)-\bar{V}_{OC})}{A_b h_c} \quad (6)$$

$$\bar{\mu}\big(T(t)\big) = k_b T(t)\, ln\left[\frac{\bar{c}}{1-c_m}\right] + \frac{\tilde{\Omega}(T(t))(c_m-\bar{c})}{c_m} - \frac{KV_S}{c_m}\bar{\nabla}^2\bar{c} \quad (7)$$

Assuming that the ion activity in the electrolyte adjacent to the particle (based on the dimensionless ion concentration) is 1.0, $\Delta\varphi_{eq} = -\frac{\mu}{e}$ provides the voltage profile for the single-particle battery $V = V^{\theta} + \eta - \frac{\mu}{e}$, where V^{θ} is the standard potential defined by the half-cell voltage (3.42 V vs. Li metal). The solution for η gives the voltage response of the single-particle battery as

$$V + V^{\theta} = \eta = \frac{\mu}{e} = \frac{k_b T}{e}\left(-\bar{\mu} - 2\, sinh^{-1}\left(\frac{\bar{I}}{\bar{I}_0(\bar{c})}\right)\right) \quad (8)$$

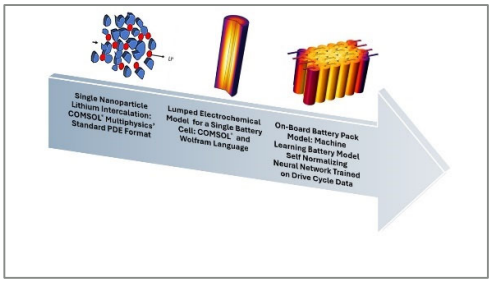

Figure 3. Multi-physics and multi-scale model and simulations.

2.2 Generating the Dataset from the COMSOL® Multiphysics Simulation

To create the simulation dataset over a broad range of conditions, we ran the COMSOL® Multiphysics simulation parameter sweep for twenty combinations of temperatures ranging from 253 to 298 K and discharge rates ranging from 1 C to 20.6 C. The SNN was coded in the Wolfram language as a Mathematica® notebook. We used PCA to determine the minimum number of features for the ROM from the simulation dataset that adequately fit the experimental data.

The raw data was standardized for a mean of 1.0 and a standard deviation of 0 resulting in an initial dataset consisting of a 1000 by 20 rectangle matrix (A). The covariance matrix (M) was then given as

$$M = \frac{A^T \cdot A}{N} \tag{9}$$

Where N is the length of the column vectors in A. We used singular value decomposition (SVD) to decompose M as

$$M = U \cdot \Sigma \cdot V^T \tag{10}$$

Substitution of the R.H.S. of Equation 10 for A in Equation 9 and simplifying gives

$$M = \frac{V \cdot \Sigma^2 \cdot V^T}{N} \tag{11}$$

Which gives the principal components as

$$A \cdot V = U \cdot \Sigma \tag{12}$$

Based on the magnitude of the singular values on the diagonal of Σ, approximately 99% of the variance was captured by the first five principal components. Projection of the original scaled data into this reduced space by

$$A_{reduced} = A_{1000X20} \cdot PC_{20X5} \tag{13}$$

gave a 1000 x 5 training set for the SNN.

3. Results and Discussion

The SPM is the simplest physics based electrothermal model for lithium-ion batteries. The model incorporates three basic physical phenomena: lithium transport in the particles, the thermodynamic relationship between lithium concentration and electrode potential, and the overpotential required to drive the lithium intercalation reactions. The terminal voltage predicted by the SPM does not include any contributions from the electrolyte and these contributions are typically only negligible when the cell is operating in a low current regime. Our SPM implemented in COMSOL® Multiphysics was motivated by (Zeng & Bazant, 2013) but we extended their results of voltage plateau estimation and used machine learning to extend the SPM to high current EV applications. The SPM alone is not capable of modeling the high current responses demonstrated by our ROM. Several authors have applied machine learning to SPM solutions, but we are first to apply machine learning to the Cahn-Hilliard phase field SPM. Another major enhancement of our single-particle model (SPM) is that it is a multiphysics, thermal model that fully couples the battery cell's heat transfer model. The battery cell level thermal model is a robust macro enthalpy balance for the battery cell despite the simplifying assumptions.

Feed forward neural networks (FNN) are largely regarded as being incapable of deep learning of abstract latent variables. However recent developments have shown that self-normalizing FNN (SNN) are capable of deep learning and are of particular use for classification and regression of tabular numeric data. SNN employs scaled exponential linear units (SELU) for activation functions. SELU have self-normalizing properties that make it possible to train deep FNN for robust learning. We minimized the size of the SNN using PCA. The resulting ROM implemented as a SNN is computationally competitive with an ECM while maintaining the first principal model authenticity via the SPM simulation. The principal components are a reduced order set of latent variables hidden in the original dataset. The latent variables are linear combinations of the column vectors in the original, larger simulation dataset. As shown in Figure 4, our SNN is a FNN with eight hidden layers with three nodes per layer, consisting of eight linear layers, seven elementwise SELU layers, seven Dropout layers and one SoftMax layer. The SNN has a rank five vector input and a scaler output of voltage.

We tested and verified the SNN for a 1 C discharge rate for ambient temperatures ranging from 253 to 298 K, as shown in Figure 5. Also, in Figure 6, the model results are compared to the experimental results for discharge rates ranging from 1.0 to 10.6 C for an ambient temperature of 298 K. Finally, we tested the trained SNN predictor function using the harsh road test dataset: Up Mount Sano in Huntsville, AL as shown in Figure 7.

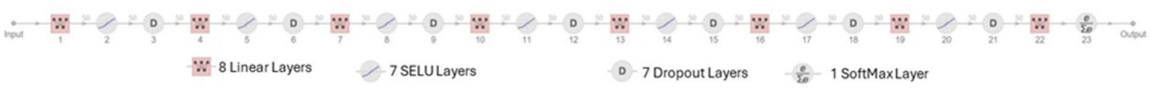

Figure 4: Schematic for the SNN

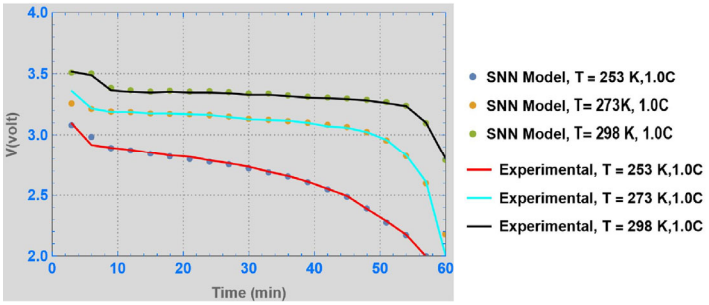

Figure 5: SNN verification for ambient temperatures 253 to 298 K.

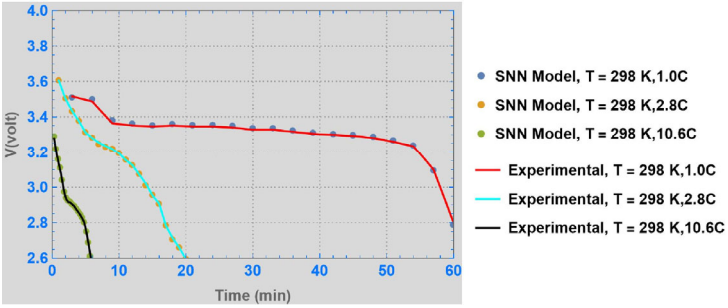

Figure 6: SNN verification for discharge current ranging from 1.0 C to 10.6 C

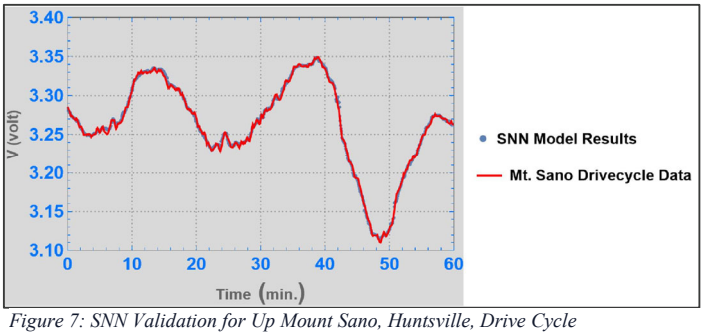

Figure 7: SNN Validation for Up Mount Sano, Huntsville, Drive Cycle

Nomenclature and Definitions

$\bar{c}$	Dimensionless concentration	Variable	$\frac{c}{c_m}$
c_m	Maximum concentration	Parameter	1.379×10^{28} [m^{-3}]
c_p	Specific heat coefficient	Parameter	825 J [k_g^{-1} K^{-1}]
h_c	Convection heat transfer coefficient	Parameter	5.0 [W m^{-2} K^{-1}]
I	Current	Variable	[A]
$\bar{I}$	Dimensionless current	Variable	$\frac{R_p}{c_m n e D_0} I$
I_0	Current density	Parameter	1.6×10^{-4} [A m^{-2}]
$\bar{I}_0$	Dimensionless current density	Parameter	$\frac{R_p}{c_m n e D_0} I_0$
k_b	Boltzmann constant	Constant	3.13×10^9 [eV K^{-1}]
$\bar{q}$	Dimensionless radial flux	Variable	$\frac{R_p}{c_m D_0} q$
$\dot{q}_{surr}$	Heat loss to surroundings	Variable	[W]
T	Temperature	Variable	[K]
T_{surr}	Surroundings temperature	Parameter	(253–298) [K]
V	Voltage	Variable	[V]
$\bar{V}$	Dimensionless voltage	Variable	$\frac{eV}{k_b T}$
$V_{c\left(\frac{1}{2}\right)}$	Voltage for half-filled particle	Variable	[V]
$V_{c\left(\frac{1}{2}\right)est}$	Cell voltage at 50 % SOC	Variable	[V]
V^{θ}	Reference voltage	Constant	3.42 [V]
V_{CH}	Voltage simulated by the SPM	Variable	[V]
$\bar{V}^{\theta}$	Dimensionless reference voltage	Constant	$\frac{eV^{\theta}}{k_b T}$
α	Electron transfer symmetry factor	Parameter	0.5
η	Activation potential	Variable	-
$\bar{\eta}$	Dimensionless activation potential	Variable	$\frac{e}{k_b T}\eta$
μ	Chemical potential	Variable	[eV]
$\bar{\mu}$	Dimensionless chemical potential	Variable	$\frac{\mu}{k_b T}$
$\frac{k_b T}{e}\mu$	Potential energy term from the SPM	Variable	-
$\frac{k_b T}{e}\bar{\mu}_{est}$	Potential energy	Variable	-
V_{OC}	Open circuit voltage		
Ω	Enthalpy of mixing	Parameter	0.115 [eV]

References

1. Tian, J.; Xiong, R.; Shen, W. Electrode aging estimation and open circuit voltage reconstruction for lithium-ion batteries. Energy Storage Mater. 2021, 37, 283–295.
2. Tian, J.; Xiong, R.; Shen, W.; Lu, J. State-of-charge estimation of LiFePO4 batteries in electric vehicles: A deep-learning enabled approach. Appl. Energy 2021, 291, 116812.
3. Etacheri, V.; Marom, R.; Elazari, R.; Salitra, G.; Aurbach, D. Challenges in the development of advanced Li-ion batteries: A review. Energy Environ. Sci. 2011, 4, 3243–3262.

4. Lu, L.; Han, X.; Li, J.; Hua, J.; Ouyang, M. A review on the key issues for lithium-ion battery management in electric vehicles. J. Power Sources 2013, 226, 272–288.
5. Dai, H.; Jiang, B.; Hu, X.; Lin, X.; Wei, X.; Pecht, M. Advanced battery management strategies for a sustainable energy future: Multilayer design concepts and research trends. Renew. Sustain. Energy Rev. 2021, 138, 110480.
6. Wang, Y.; Tian, J.; Sun, Z.; Wang, L.; Xu, R.; Li, M.; Chen, Z. A comprehensive review of battery modeling and state estimation approaches for advanced battery management systems. Renew. Sustain. Energy Rev. 2020, 131, 110015.
7. Scrosati, B.; Garche, J. Lithium Batteries: Status, Prospects and Future. J. Power Sources 2010, 195, 2419–2430.
8. Fergus, J. Recent Developments in Cathode Materials for Lithium-Ion Batteries. J. Power Sources 2010, 195, 939–954.
9. Shim, J. Electrochemical analysis for cycle performance and capacity fading of a lithium-ion battery cycled at elevated temperature. J. Power Sources 2002, 112, 222–230.
10. Ning, G.; Popov, B. Cycle Life Modeling of Lithium-Ion Batteries. J. Electrochem. Soc. 2004, 151, A1584.
11. Spotnitz, R.; Franklin, J. Abuse behavior of high-power, lithium-ion cells. J. Power Sources 2003, 113, 81–100.
12. Li, Y.; Karunathilake, D.; Vilathgamuwa, D.M.; Mishra, Y.; Farrell, T.W.; Zou, C. Model Order Reduction Techniques for Physics-Based Lithium-Ion Battery Management. *IEEE Ind. Electron. Mag.* **2022**, *16*, 36–51.
13. Painter, R.; Embry, I.; Sharpe, L.; Hargrove, S.K. A Reduced Order Thermal Model for Lithium-Ion Batteries Derived from the Cahn-Hilliard Equation. In Proceedings of the 2020 COMSOL® Conference, Boston, MA, USA, 7–8 October 2020.
14. Bai, P.; Cogswell, D.; Bazant, M.Z. Suppression of phase separation in $LiFePO_4$ nanoparticles during battery discharge. *Nano Lett.* **2011**, *11*, 4890–4896.
15. Zeng, Y.; Bazant, M. Cahn-Hilliard Reaction Model for Isotropic Li-Ion Battery Particles. *MRS Proc.* **2013**, *1542*, 0201.
16. Singh, S.;Weeber, M.;Birke, K. Implementation of digital twin: Approach, Functionaliyies and Benefits, Batteries, MDPI, 2021.